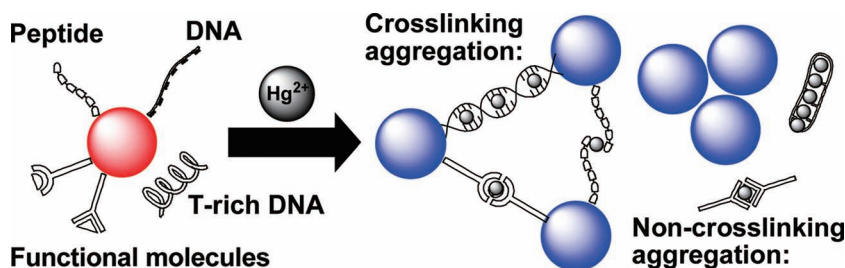


Colorimetric Detection of Mercury Ions Based on Plasmonic Nanoparticles

Jianjun Du, Lin Jiang, Qi Shao, Xiaogang Liu, Robert S. Marks, Jan Ma, and Xiaodong Chen*



From the Contents

1. Introduction	1468
2. Correlation between Colorimetric Detection and Plasmonic Nanoparticles	1468
3. Oligonucleotide-AuNP Probes	1469
4. Oligopeptide-AuNP Probes	1473
5. Functional Molecule-AuNP Probes	1474
6. Multiple Signal Amplification	1477
7. Conclusion and Outlook	1478

The development of rapid, specific, cost-effective, and robust tools in monitoring Hg^{2+} levels in both environmental and biological samples is of utmost importance due to the severe mercury toxicity to humans. A number of techniques exist, but the colorimetric assay, which is reviewed herein, is shown to be a possible tool in monitoring the level of mercury. These assays allow transforming target sensing events into color changes, which have applicable potential for in-the-field application through naked-eye detection. Specifically, plasmonic nanoparticle-based colorimetric assay exhibits a much better propensity for identifying various targets in terms of sensitivity, solubility, and stability compared to commonly used organic chromophores. In this review, recent progress in the development of gold nanoparticle-based colorimetric assays for Hg^{2+} is summarized, with a particular emphasis on examples of functionalized gold nanoparticle systems with oligonucleotides, oligopeptides, and functional molecules. Besides highlighting the current design principle for plasmonic nanoparticle-based colorimetric probes, the discussions on challenges and the prospect of next-generation probes for in-the-field applications are also presented.

1. Introduction

Mercury is one of the most toxic and dangerous heavy metal elements to human health and environmental safety. Mercury contamination is toxic and widespread through various natural and anthropogenic processes, such as volcanic emissions, mining, solid waste incineration, and combustion of fossil fuels.^[1] Subsequent bioaccumulation through the food chain can lead to severe damage to many important organs such as the brain and kidney, as well as deleterious effects on human health in the forms of dysphoria, tremors, vegetative nerve functional disturbance and so on.^[2] The World Health Organization (WHO) standard for the maximum allowable level of inorganic mercury in drinking water is no more than 6 ppb (30 nM).^[3] Thus, concerns over the safety of drinking water, damage associated with mercury toxicity, and its toxicology, have provided the motivation to develop rapid, specific, cost-effective, and robust tools for monitoring ionic mercury (Hg^{2+}), which is one of most stable and widespread inorganic forms of mercury in the environment and organisms.

Although conventional analytical approaches for Hg^{2+} analysis, such as atomic absorption spectroscopy,^[4] inductively coupled plasma mass spectrometry,^[5] and selective cold vapor atomic fluorescence spectrometry^[6] could provide qualitative and quantitative information, they are rather costly, complex, time-consuming, non-portable, and require specialized laboratories. One should note that these methods give accurate and sensitive quantification of the total amount of metal present in the sample. However, before using these analytical methods, environmental samples require laborious treatment to solubilize the metal ions from the solid matrix (i.e., soils or sediments which are sinks for released metals). Still, a simplification of these techniques would be a welcome event.^[7] Therefore, a variety of remarkable probes based on organic molecules,^[8] polymeric materials,^[9] biomaterials,^[10] semiconductor nanocrystals,^[11] and agglutination materials^[12] have been developed for Hg^{2+} detection over the past decades, which normally test Hg^{2+} using optical and electrochemical signals.^[13] However, most of examples are not well suited for on-field analysis or rapid screening. Alternatively, colorimetric detection, a method of determining the existence and concentration of an analyte with the aid of an obvious color change is particularly attractive for point-of-use applications due to its simple readout by the naked eye. In recent years, a variety of organic chromophoric probes have been utilized in monitoring metal ions,^[14] anions,^[15] thiols,^[16] amino acids,^[17] nucleotides,^[18] and explosives.^[19] However, their sensitivity, solubility, and assay range usually limit the application of organic chromophoric probes.^[20] A new field has been developing rapidly to provide a possible solution to the unsatisfied criteria for colorimetric detection. Indeed, plasmonic nanoparticle-based colorimetric detection is drawing increasing attention, as it could overcome the difficulties mentioned above.

Plasmonic nanoparticles, such as gold nanoparticles (AuNPs) and silver nanoparticles (AgNPs), are a class of nanostructures whose optical properties are determined by

their unique surface plasmon resonances (SPRs).^[21] Unlike propagating plasmons supported on a bulk metal surface, nanoparticle plasmons are the collective oscillations of their conduction electrons confined to nanoscale volumes upon light irradiation (incident electromagnetic waves). Such resonance is sensitive to nanoparticle size, shape, interparticle distance, and local dielectric environment.^[22] So far, various nanoparticles with different sizes and shapes have been developed for diverse applications. Since they have good stability and low toxicity,^[23] several AuNP-based colorimetric assays have been designed, prepared, and widely applied in detecting DNA,^[24] enzyme activity,^[25] proteins,^[26] small molecules,^[27] anions/metal ions,^[28] and so on.

The purpose of the present review is to summarize the progress in the design and application of AuNP-based colorimetric assays for Hg^{2+} . We begin with a brief discussion on the correlation between colorimetric detection and plasmonic nanoparticles. Then, we describe the general design principles that govern the nanoparticle-based colorimetric assays for Hg^{2+} detection. They are classified according to the type of functional decorators on nanoparticles such as oligonucleotides, oligopeptides, and functional molecules (**Figure 1**). Furthermore, the combination of multiple signal amplification together with AuNPs for enhanced sensitivity is introduced. Lastly, we present our views on the future outlook of plasmonic nanoparticle-based colorimetric detection for on-field applications.

2. Correlation between Colorimetric Detection and Plasmonic Nanoparticles

There are essentially two key components of a colorimetric assay that affect the performance in selectivity, sensitivity, response time, and signal-to-noise ratio. One is the recognition moiety that provides a selective/specific response to the analyte, which relates to a wide range of organic or biological ligands/reactions. The other is the transducer moiety

Dr. J. Du, Dr. L. Jiang, Q. Shao, Prof R. S. Marks,
Prof. J. Ma, Prof. X. Chen
School of Materials Science and Engineering
Nanyang Technological University
50 Nanyang Avenue, 639798, Singapore
E-mail: chenxd@ntu.edu.sg

Prof. X. Liu
Department of Chemistry
National University of Singapore
3 Science Drive 3, 117543, Singapore
Institute of Materials Research and Engineering
A*Star, 3 Research Link, 117602, Singapore

Prof. R. S. Marks
Department of Biotechnology Engineering
National Institute for Biotechnology in the Negev
and the Ilse Katz Center for Meso and
Nanoscale Science and Technology
Ben-Gurion University of the Negev
Beer-Sheva, 84105, Israel

DOI: 10.1002/sml.201200811



that translates detecting behavior into an eye-sensitive color change in the range of 390 to 750 nm.

Plasmonic nanostructures have the ability to support surface plasmons (Figure 2a)^[21a] that are generated by the coupling between incident electromagnetic waves with the conduction electrons in metal nanostructures.^[29] These kinds of plasmons normally occur in AuNPs and AgNPs with a size range of 10–200 nm and result in an amplification of the electromagnetic field near the particle surface. By tailoring the size, shape, and environment of metal nanostructures, the SPR adsorption of nanostructures can be tuned. In addition, when nanostructures approach one another (i.e., when they aggregate), the SPR bands are dramatically altered as a result of the strong coupling between the localized SPRs of the nanostructures.^[21b,21c]

Many plasmonic nanostructures with various sizes, shapes (rod, cube, disc, etc.), and structures (shell, core-shell, cage, tube, etc.) have been developed,^[30] which enable the tailoring of their SPR adsorption. For instance, the shape and size of AgNPs can be controlled either photochemically by adjusting the wavelength of irradiation or chemically by varying the pH of the reaction solution.^[31] As a result, a large range of SPR absorption bands were obtained from visible region to near infrared region (Figure 2b,c). For example, AuNPs with the diameter of 10–50 nm usually appear ruby red in the solution. When AuNPs aggregate, a dramatic red-to-blue color change can be clearly observed, since the SPR adsorption displays a red shift, broadening and decreasing in intensity compared with that of isolated nanoparticles. Among various plasmonic nanoparticles, AuNPs are most suitable for naked-eye colorimetric detection because changes between red and blue are dramatic and readily detected by human eyes, which lead to their extensive application.

There are six main advantages to AuNP-based colorimetric detection compared to organic chromophoric probes:^[32] 1) ease of synthesis with high dispersity in aqueous media; 2) greater absorption extinction coefficient (ca. $10^8 \text{ cm}^{-1} \text{ M}^{-1}$ for AuNPs) compared to that of common organic dyes (ca. $10^5 \text{ cm}^{-1} \text{ M}^{-1}$); 3) strong photostability; 4) ease of physical and chemical functionalization through suitable surface chemistry; 5) a large surface-to-volume ratio with unusual target-binding properties, and; 6) alterable optical properties (e.g., SPR) which directly relate to the size, shape, and composition of the nanoparticles, and their interparticle distance. Therefore, AuNP-based colorimetric assays have been successfully designed and widely applied.

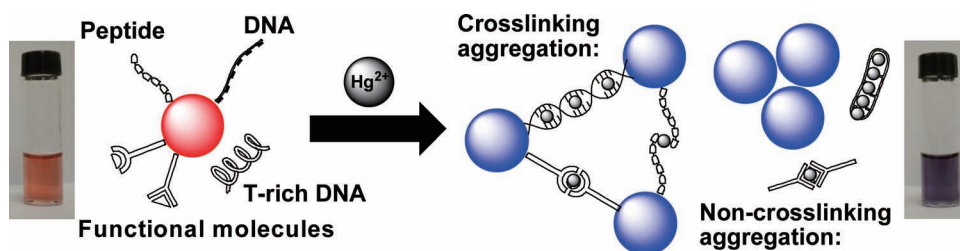
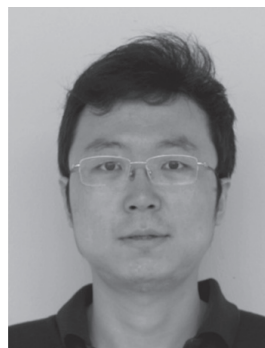


Figure 1. Schematic illustration of AuNPs based colorimetric probe.



Jianjun Du is a Research Fellow at the School of Materials Science and Engineering, Nanyang Technological University (Singapore). He received his BS degree in Chemistry from Dalian University of Technology (China) in 2004, and obtained his PhD from Dalian University of Technology (China) in 2010. He is presently working as a postdoctoral fellow in the group of Prof. Xiaodong Chen. His research is focused on fluorogenic and colorimetric probes based on organic and inorganic materials.



Xiaodong Chen is a Singapore National Research Foundation (NRF) Fellow and Nanyang Assistant Professor at the School of Materials Science and Engineering, Nanyang Technological University (Singapore). He received his BS degree (Hons) in Chemistry from Fuzhou University (China) in 1999, MS degree (Hons) in Physical Chemistry from the Chinese Academy of Sciences in 2002, and PhD degree (Summa Cum Laude) in Biochemistry from University of Muenster (Germany) in 2006. After his postdoctoral fellow working at Northwestern University (USA), he started his independent research career at Nanyang Technological University in 2009. His research interests include the integrated nano-bio interface and bio-inspired nanomaterials for energy conversion.

3. Oligonucleotide-AuNP Probes

Oligonucleotide-AuNP probes have been widely used in the field of bio-nanotechnology for diagnosis and therapy^[24a,33] due to their unique chemical and physical properties.^[34] For instance, both quantitative and qualitative detection of various targets through precise and reversible control of the aggregation of nanoparticles have been utilized as powerful diagnostic platforms to detect target analytes such as proteins,^[35] polynucleotides,^[33a,36] metal ions,^[37] and small molecules.^[38] In the following sections, we will discuss how the oligonucleotide-AuNP probes are designed for detecting Hg²⁺.

3.1. dsDNA-AuNP Probes

In general, mixing two kinds of AuNP probes functionalized with complementary ssDNA sequences would result in the

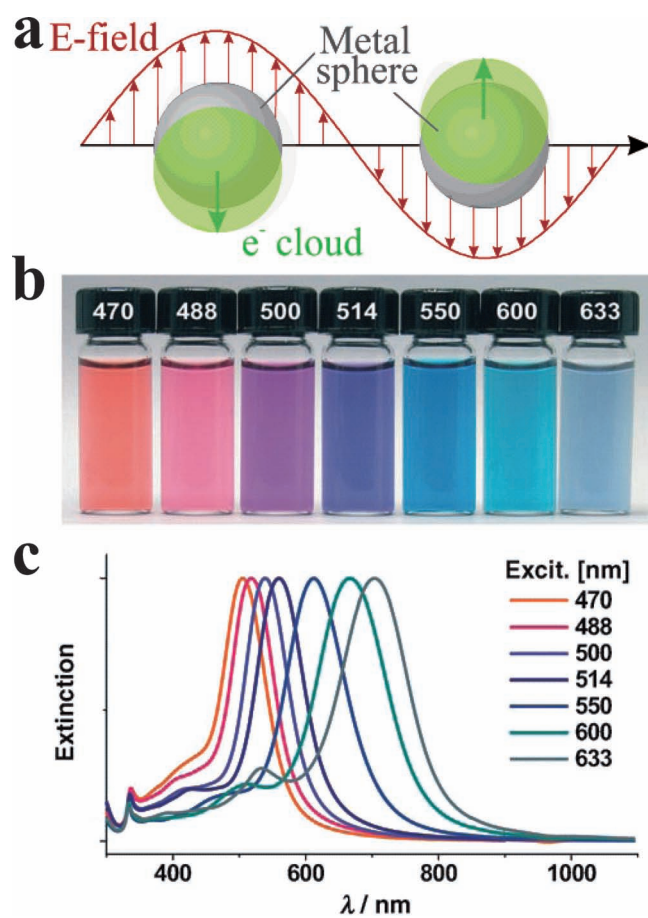


Figure 2. (a) Schematic of plasmon oscillation for a sphere, showing the displacement of the conduction electron charge cloud relative to the nuclei. Reproduced with permission.^[21a] Copyright 2003, The American Chemical Society. (b,c) Size- and shape-tunable surface plasmon resonance spectra of various AgNPs. Reproduced with permission.^[31]

polymeric network-like aggregation of AuNPs accompanied by a red-to-blue color change because of the red shift of the SPR adsorption band.^[24a,33a,39] Interestingly and importantly, this process is reversible upon heating, which can de-hybridize dsDNA along with the recovery of the original absorption and color. The melting profiles of the complementary duplex DNA strands labeled on AuNPs exhibit an extraordinarily sharp transition compared to that of free DNA strands.^[40] Dependent on thymine-Hg²⁺-Thymine (T) coordination chemistry, the colorimetric assay for Hg²⁺ was first introduced and subsequently developed by the Mirkin group based on a complementary DNA-AuNP system with designed T-T mismatches.^[41] As shown in **Figure 3a**, two types of nanoparticles aggregated together after the specially designed ssDNA hybridized, causing a red-to-purple color change. After raising the temperature to the melting temperature, T_m , the dsDNA de-hybridized, which made AuNP aggregates dissociate reversibly along with a color change back to red. Among environmentally relevant metal ions (Mg²⁺, Pb²⁺, Cd²⁺, Co²⁺, Zn²⁺, Fe²⁺, Ni²⁺, Fe³⁺, Mn²⁺, Ca²⁺, Ba²⁺, Li⁺, K⁺, Cr³⁺, Cu²⁺, and Hg²⁺), only Hg²⁺ could raise the T_m obviously (ca. 5 °C) as

shown in **Figure 3b**. The sharp melting transition enhanced the sensitivity and lowered the limit of detection (LOD) visibly to 100 nM (20 ppb) in contrast to organic colorimetric system (LOD: usually in ppm range). Initially, dsDNA-AuNP probes were developed for studying the imperfect DNA targets (such as single base mismatch or mutations),^[24a,36] as it is known that the T_m is decreased in the presence of base mismatches or mutations in DNA strands.^[42] A point to note is that complementary DNA strands together with T-T mismatches can form a duplex DNA, creating a T-Hg²⁺-T complex, thanks to Hg²⁺, which selectively bridges two thymine molecules in a stable manner.^[43] Such a unique structure can obviously increase the T_m in such a way that the melting analysis could be used for qualitative determination. One can design a smart, tailored ssDNA-AuNP system, which could provide the user with notable selectivity toward Hg²⁺ without significant interference from other metal ions. In addition, this system takes advantage of the sensitivity provided by AuNPs and thus, together, these properties can be considered an improvement over traditional probes for Hg²⁺ detection. Nonetheless, heating is needed in this assay for thermal denaturation of dsDNA and the temperature change should be monitored carefully, which impedes fast sample detection in practice.

Based on the initial work of the Mirkin group, Liu et al. developed a system that was not only selective and sensitive but also practical and convenient for colorimetric detection of Hg²⁺ at room temperature.^[44] Their studies showed that the extent of reduced T_m was proportional to the amount of T-T mismatch and therefore taking advantage of this fact, the T_m could even be further reduced below the operating ambient temperature (23 °C) when the T-T mismatch amount reached 8 (probes A*, B, and C; $T_m = 14.4$ °C, **Figure 3d**). Generally, in order to detect target oligonucleotides for the diagnosis of gene-pathogenic diseases, a three-ssDNA system is now preferred^[36,45] wherein two different probe ssDNAs have been carefully designed and functionalized to AuNPs respectively as probe **A** and **B**, and together they complementarily recognize different parts of the third target ssDNA (**C**) by forming stable dsDNA. It is inferred that T_m would become lower and lower along with an increase of base mismatches, and that these probes could even finally not hybridize when the T_m is lower than the operating temperature. However, in the case where the mismatches are all T-T type, probe **C** would recognize and hybridize both particle probe **A** and **B** via the formation of stable dsDNA in the exclusive case that Hg²⁺ is present in the solution at a given operating temperature. Therefore, colorimetric detection of target Hg²⁺ at room temperature is achieved through the systematic control and optimization of the amount of T-T mismatches within the probe **C** and **A/B** system (**Figure 3c,d**), which renders the heating and T_m monitoring steps redundant. Thus a rapid detection of Hg²⁺ is shown that is selective to a single metal ion and that provides a good sensitivity at room temperature.

Furthermore, Takarada et al. demonstrated that T-T mismatches in different positions could lead to differences in the change of T_m (**Figure 3e**).^[46] Different positions of T-T mismatches in dsDNA were studied at the distal end, penultimate, and antepenultimate positions. The results showed

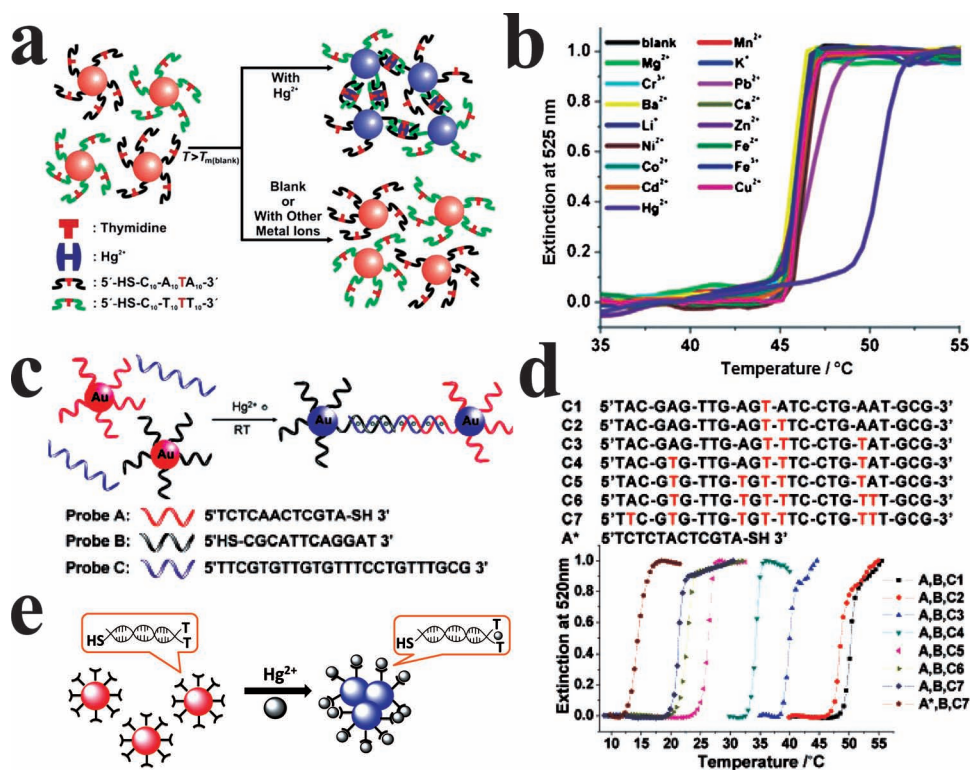


Figure 3. (a) Schematic representation of colorimetric detection of Hg^{2+} using ssDNA-AuNPs and (b) their normalized melting curves of aggregates in the presence of various metal ions. Reproduced with permission.^[41] (c) Schematic representation of colorimetric detection of Hg^{2+} using ssDNA-AuNPs and (d) their normalized melting curves of solutions containing probes A (or A*), B, and the linker probes C₁₋₇ with varied T-T mismatches. Reproduced with permission.^[44] Copyright 2008, The American Chemical Society, and; (e) schematic illustration of spontaneous aggregation of dsDNA-carrying AuNPs with T-T mismatch in terminal.

that T-T mismatches in different positions could lead to varying changes of T_m and thus different LODs could be obtained. One of the best visual LODs reached was, at 0.5 μM Hg^{2+} , using a system with T-T mismatches at the antepenultimate position. This system exhibited good selectivity to Hg^{2+} in 1 min without having to control the temperature or mask reagents. In media with high ionic strength, fully matched dsDNA tethered on the surface of AuNPs can stabilize nanoparticles to some extent, because of the steric hindrance from dsDNAs. However, dsDNA with base mismatches in the terminal end would form branch-type structures, which cause much more steric hindrance and larger entropic repulsion than that of the rigid structures, resulting in much higher colloidal stability for dispersions in identical saline solutions.

It is known that free, non-tethered ssDNA (without a thiol modification at its end) can also attract AuNPs and form complexes because of the coordination between Au and the nitrogen atoms in DNA bases.^[47] However, dsDNA cannot follow such a behavior because DNA bases are concealed after the hybridization event, while the negative phosphate backbone is exposed. Based on these facts, Yang et al. presented examples of a new system based on colorimetric and fluorescent dual sensing where Hg^{2+} was coordinated within a dye-tagged ssDNA with T-T mismatch sequences (**Figure 4**).^[48] Fluorescein (FAM)

was introduced as the fluorescence source, as its emission at 518 nm has a good overlap with the SPR band of AuNPs (13 nm) at 520 nm; therefore, more than 95% quenching could be observed through a fluorescence resonance energy transfer (FRET) process. In the absence of Hg^{2+} , the dye-tagged ssDNA (sequence 2, Figure 4b) that was absorbed on the surface of AuNPs via an electrostatic effect, protected the particles from aggregation at high ionic strengths and the FAM's fluorescence was quenched at the same time. In the presence of Hg^{2+} , sequence 2, rich in thymine bases and labeled with FAM at the 3'-end, could form dsDNA with sequence 4 through vehicular Hg^{2+} and subsequently detach from the surface of the AuNPs. As a result, fluorescence was returned, accompanied by a red-to-blue color change owing to the non-crosslinking aggregation of AuNPs. This example is similar to the molecular beacon system consisting of a fluorescent dye and a corresponding quencher in both ends of ssDNA, which is used for trapping DNA targets for tailored FRET-based detection. In Yang's system, however, only the dye labeled ssDNA is needed, resulting in less laborious and more cost-effective synthesis compared to the known molecular beacon system, since the AuNPs themselves are good fluorescence quenchers. In addition, neither a covalent tether of AuNPs with oligonucleotides nor a subsequent purification is required, which makes the system more efficient for practical applications.

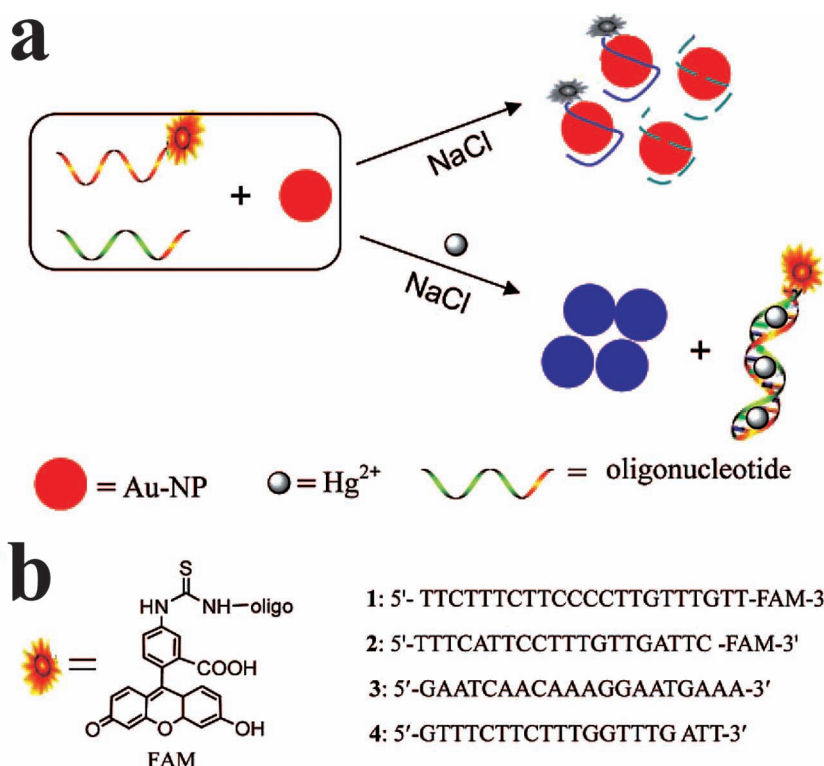


Figure 4. (a) Schematic depiction of colorimetric and fluorescent sensing of Hg²⁺ based on the free AuNPs and (b) structures of fluorescein (FAM) and the FAM-labeled ssDNAs. Reproduced with permission.^[48] Copyright 2008, The American Chemical Society.

Three types of DNA-AuNP modes have been summarized at this point: 1) a AuNP-dsDNA-AuNP mode, wherein both ends of a dsDNA are tethered on different nanoparticles through Au-S bonds; 2) a dsDNA-AuNP mode, wherein only one side of the dsDNA is tethered on the nanoparticle, and; 3) a dsDNA/Au mode, wherein the DNA is totally free. Furthermore, in the exclusive case of the development of AuNPs based Hg²⁺ probes, one can summarize the systems as follows: 1) compared to a typical ssDNA tethered AuNP system, the free ssDNA/AuNP system provides a more cost-effective, simple, and rapid determination for Hg²⁺ when based on a non-crosslinking aggregating mode, which requires neither functionalization, nor separation or purification processes; 2) with careful design, the geometry and space structure of T-rich ssDNA could be transformed from a free and uncoiled state to a specific hybridization structure (like a hairpin structure) using Hg²⁺ as a bridge (T-Hg²⁺-T) and induce the non-crosslinking-based colorimetric detection without the need to record a temperature

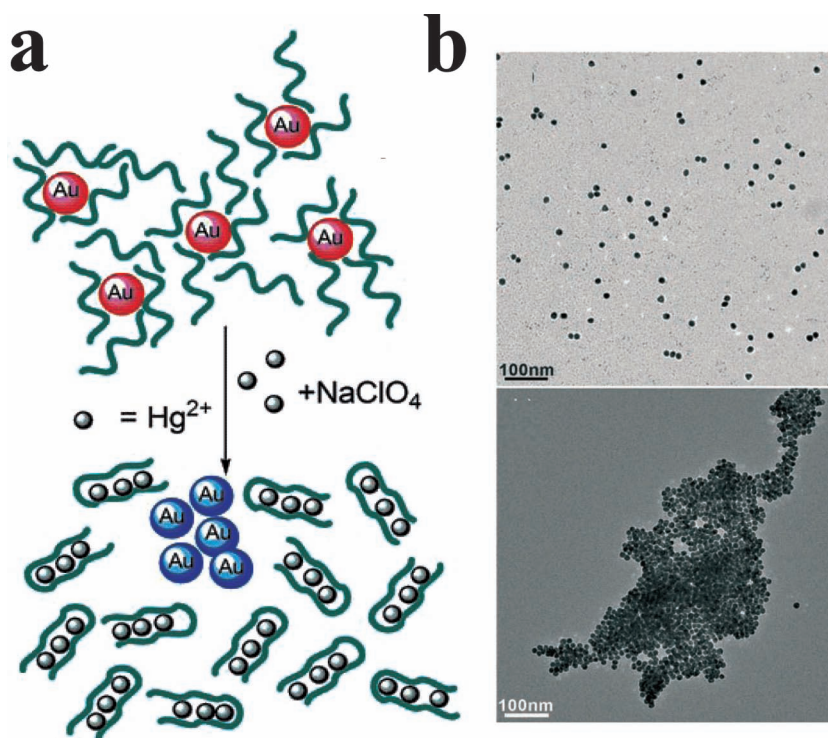


Figure 5. (a) Schematic representation of Hg²⁺ stimulated aggregation of AuNPs and (b) TEM images of non-aggregated AuNPs stabilized by ssDNA in the presence NaClO₄ and the aggregated AuNPs after addition of Hg²⁺. Reproduced with permission.^[49] Copyright 2008, Wiley.

change. Compared to well-studied ssDNA tethered AuNPs systems, free ssDNA/AuNPs systems have been well developed in recent years and show great future potential, as described in detail in the following section.

3.2. T_n-ssDNA-AuNP Probes

Simple, fast, and wide-range systems for the detection of Hg²⁺ using T_n-ssDNA have been developed. For instance, Willner et al. prepared T-rich nucleic acid (5'-TTCTTTCTTCCCCTT-GTTTGGT-3') for Hg²⁺ detection (**Figure 5**).^[49] After treating AuNPs (13 nm) with ssDNA, NaClO₄ (100 mM) was added into the solution to maintain a high level of salinity. Under this condition, red color with an absorption band at 520 nm was observed before addition of Hg²⁺, indicating good dispersion of the nanoparticles. Upon addition of Hg²⁺ the solution turned blue, induced by aggregation of AuNPs, which was detected by the naked eye and also

confirmed by a red shift and broadened peak in the UV–vis spectrum. Macroscopic changes were attributed to the formation of the nucleic acid duplex-folded complex with the help of Hg^{2+} , and following release of ssDNA from AuNPs. As a result, the system became so destabilized that AuNPs aggregated. This probe showed good selectivity to Hg^{2+} among normal metal ions except for Pb^{2+} , which could actually be masked using 2,6-pyridinedicarboxylic acid (PDCA), and analysis for Hg^{2+} could be done at concentration of 100 nM, with an LOD of 10 nM (2 ppb). In addition, Yang's group demonstrated an example based on thrombin-binding aptamer (TBA, 5'-GGTTGGTGTGGTTGG-3'), which realized an Hg^{2+} colorimetric assay with an LOD of 200 nM.^[50] These ssDNA-AuNP sensing systems further simplify the fabrication of the detecting systems and provide us with a wide detection range for Hg^{2+} . It is also found that ssDNA chains with different sequences show varying performances (like LOD) for Hg^{2+} detection, which indicate that the amount and the position of thymine are both key factors in the ssDNA-AuNP probe design.

Since the amount of thymine in ssDNA or the length of the T_n -ssDNA is directly related to the sensitivity toward Hg^{2+} , Chang et al. focused on the quantitative study by testing T_n -ssDNA at different lengths (T_7 , T_{33} , and T_{80}).^[51] It was shown that although the longer ssDNA did better in stabilizing AuNPs in the same concentration, T_{33} performed better than either T_7 or T_{80} in the detection of Hg^{2+} . This may be due to the fact that T_7 was too short to form folded structure. In contrast to this, T_{80} was considered too long to dissociate from AuNPs. Li et al. found that the aptamer T_{10} even performed better with an LOD of 0.6 nM under optimum condition (0.1 M HAc-NaAc, pH 4.0, 20 °C).^[52] Therefore, an appropriate amount of thymine should be selected when considering an equilibrium point between stabilizing AuNPs in the absence of Hg^{2+} and dissociating from AuNPs in the presence of Hg^{2+} .

The common paradigm is that fluorescence signals are more sensitive than absorption ones in sensing systems. However, it has been shown here that similar LODs for Hg^{2+} were obtained from both such signals by Li et al. using their ssDNA-AuNP systems.^[53] It is thought that some dye-tagged dsDNA remained attached to the surface of AuNPs during dissociation in the presence of Hg^{2+} . Once T-rich ssDNA bound with enough target Hg^{2+} (high concentration) and formed a dsDNA structure through T- Hg^{2+} -T complexes, increasing overall positive charges of dsDNA, some dye-labeled dsDNA bound to the AuNPs and quench themselves, before electrostatic interactions dominated and aggregation of the dsDNA/AuNPs system happened. These aforementioned results provide an additional understanding of the interactions between DNA and AuNPs in the presence of low or high Hg^{2+} concentrations.

Using a similar system involving T_n -ssDNA-AuNP for Hg^{2+} detection, Tseng et al. found that the presence of Mn^{2+} could accelerate and enhance the aggregation of AuNPs in high salt media.^[54] It was found that addition of Mn^{2+} (0.2 mM) would not affect the stability of system but could increase the sensitivity by 100-fold to achieve 10 nM (LOD) in Hg^{2+} detection. The added Mn^{2+} could stabilize the folded

structure of the T_n -ssDNA-AuNP complex, which could facilitate the release of poly-T DNA from the particle surface and speed up their aggregation. This thanks to the fact that the metal ions of Mn^{2+} coordinate with DNA bases and bind to the phosphate backbone of DNA owing to their specific ionic valence and coordination geometry.

4. Oligopeptide-AuNP Probes

Oligopeptides are the source of highly specific ligands enabling the capture of specific targets through a combination of non-covalent interactions like hydrogen bonding, ionic bonding, and π - π stacking found in 3D cavities filled with functional groups from amino acids lying at the inner or outer surfaces. Unlike DNA bases, there are about 20 kinds of natural amino acids, all of which can act as building blocks in the peptide/protein synthesis. Therefore, multiple permutations and combinations with different functions become possible, where even a tripeptide, for instance, has 20^3 kinds of possible sequences. Oligopeptides show some unique intricacies, which could be utilized in AuNP-based colorimetric systems, such as 1) hydrophobicity/hydrophilicity can be regulated by adjusting the configuration of hydrophobic and hydrophilic amino acids; 2) multiplexed readouts can supply more choices (e.g., the indol group in tryptophane fluoresces at 350 nm);^[55] 3) unlike DNA strands, multiple options in introducing more functional groups are possible, like carboxyls, aminos, hydroxyls, thiols, and so on; 4) in addition, oligopeptides also exhibit a redox capability, which could be used in the synthesis of oligopeptide-AuNPs. In the following

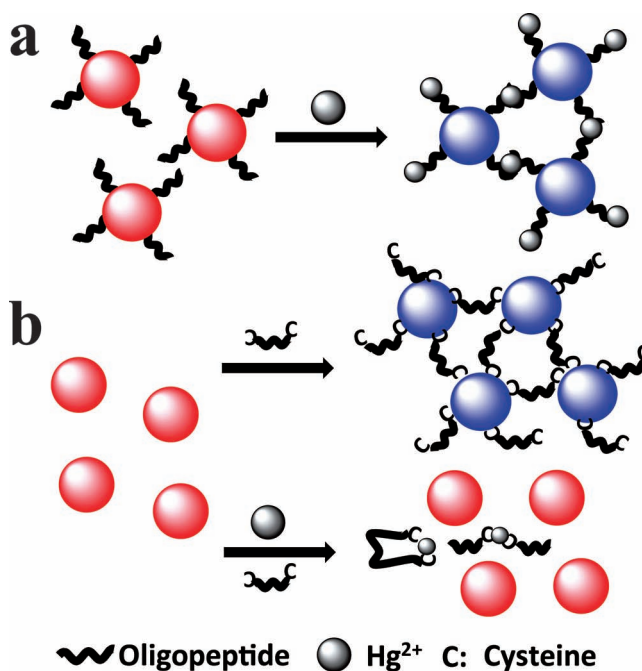


Figure 6. (a) Schematic representation of colorimetric detection of Hg^{2+} based on an oligopeptide-AuNP system; (b) colorimetric detection of Hg^{2+} based on simply mixing AuNPs and oligopeptides with cysteines at both terminals.

section, we will discuss how oligopeptide-AuNP probes work in Hg^{2+} detection.

For example, Mandal et al. prepared an oligopeptide-AuNP system ($\text{NH}_2\text{-Leu-Aib-Tyr-COONa}$) in situ by oligopeptide reduction and stabilization to work as a colorimetric assay for Hg^{2+} detection (Figure 6a).^[56] In the absence of Hg^{2+} , it showed an initial sharp and characteristic SPR band at 527 nm. Upon addition of 4 ppm Hg^{2+} , a red-to-purple color change was observed, while an additional 8 ppm Hg^{2+} brought a new SPR band at 670 nm accompanied by a red-to-blue color change. This special oligopeptide exhibited a good selectivity toward Hg^{2+} among other metallic ions such as Pb^{2+} , Cu^{2+} , Cd^{2+} , Zn^{2+} , and Ca^{2+} . More recently, Naik et al. developed a colorimetric method for detecting metal ions using oligopeptide-AuNPs.^[57] The oligopeptide (-Asp-Tyr-Lys-Asp-Asp-Asp-Lys-Pro-Ala-Tyr-Ser-Ser-Gly-Pro-Ala-Pro-Pro-Met-Pro-Pro-Phe-) was selected ($\text{pI} = 3.9$) and its functional groups did interact with metal ions, showing obvious colorimetric responses to several metal ions in addition to Hg^{2+} within a 1 min time period, exhibiting an LOD as low as 26 nM for Hg^{2+} .

Chen et al. proposed a new colorimetric Hg^{2+} assay composed of AuNPs and oligopeptides (Lys-Cys-Gly-Trp-Gly-Cys) without any pre-chemical modification of the AuNPs (Figure 6b).^[32] Thanks to a strong affinity of Hg^{2+} for cysteine groups in oligopeptides (found in nature as poisoning effects through mercury's high affinity to thiol groups in enzymes), a strong ionic selectivity was obtained. In order to span a wide detecting range of Hg^{2+} (from a nanomolar to a millimolar level) that would encompass the USA Environmental Protection Agency (EPA) standards for both industrial wastewater (250 nM; 50 ppb) and drinking water (10 nM; 2 ppb), one would imagine having an array of different amounts of oligopeptides based on the estimated concentration of Hg^{2+} . Adding linear oligopeptides with Cys at both ends into a solution containing AuNPs will provoke their aggregation, as evidenced by a color change from red to blue. Hg^{2+} preferentially reacts with thiolates because Hg^{2+} and Cys have a significantly higher affinity than that of Au-Cys. Thus, the solution of AuNPs remains stable and red, which avoids false positives due to spontaneous particle aggregation.

The cases just described illustrate not only the potential of these systems but also the fact that multiplicity of oligopeptides from a multitude of sequential combinations would open the opportunity to create a large number of applications.

5. Functional Molecule-AuNP Probes

One may imagine a variety of functional molecules, in addition to oligonucleotides and oligopeptides, that could

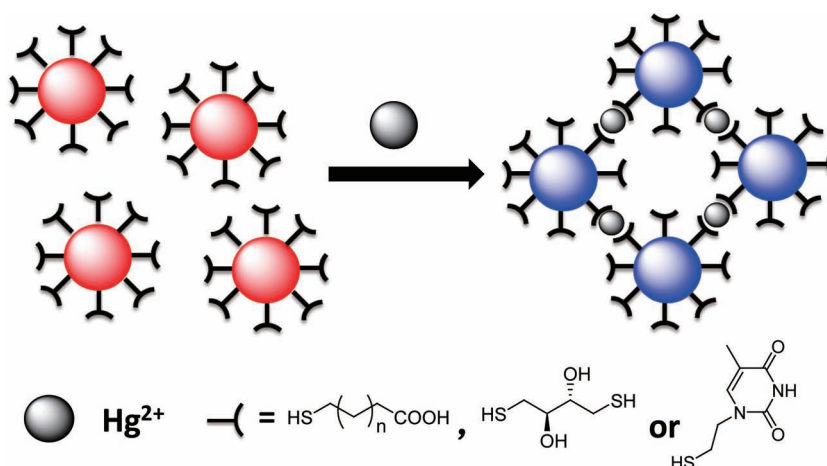


Figure 7. Schematic representation of colorimetric detection for Hg^{2+} based on functional molecules decorated AuNPs.

also be introduced into AuNP-based systems, which would either stabilize or aggregate the nanoparticles via covalent binding, electrostatic attraction, or repulsive interactions. The functional molecules have the potential to be superior to oligonucleotides and oligopeptides, through simplicity, convenience, and multiplicity. Their design philosophy and methodology in creating specific functional interactions of molecule-target and molecule-AuNP rely on surface chemistry, colloid chemistry, and coordination chemistry as found in the organic chromogenic and fluorescent probes field. The framework of decorator-AuNPs includes: 1) coordination-based systems, in which specific ligands are functionalized on the surface of AuNPs through chemical grafting (like S-Au bonds), the electrostatic effect, or physical adsorption, and; 2) chemodosimeter-based systems, wherein the state of AuNPs would be affected by the reaction.

5.1. Coordination based Functional Molecule-AuNP Probes

Thiol is one of the main functional groups for tethering to the surface of AuNPs due to the strong Au-S bond. Functional groups with O, N, and S atoms also play important roles in ligands, such as in carboxyls, aminos, hydroxyls, as well as thiol groups. Therefore, derivatives of mercapto aliphatic acid become preferred decorators for an AuNP system. As early as 2001, Tupp et al. employed 11-mercaptoundecanoic acid (MUA)-capped AuNPs (13 nm) as colorimetric sensors for heavy metal ions (Figure 7).^[58] Aqueous suspensions of MUA-capped AuNPs displayed intense SPR absorptions centred at 526 nm, which rendered the solution red. Since the recognizing moiety just involved carboxyl groups, this system showed comprehensive chelation to several heavy metal ions, such as Pb^{2+} , Cd^{2+} , and Hg^{2+} . Aggregation of the particles induced by those metal ions yielded both a shift in the SPR band and a substantial increase in long-wavelength Rayleigh scattering, which in turn led to a visual color change from red

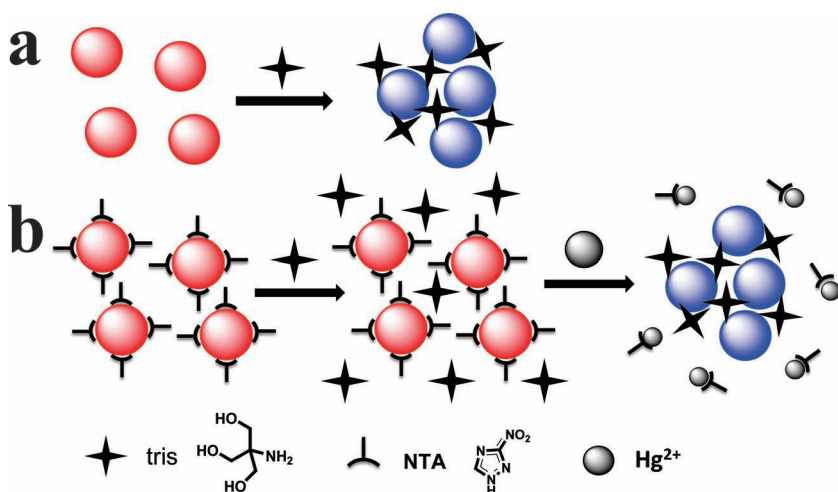


Figure 8. Schematic representation of Hg^{2+} detection based on NTA-capped AuNPs.

to blue. Subsequently, Chang et al. used 3-mercaptopropionic acid (MPA) for Hg^{2+} detection.^[59] Results showed that this system exhibited a higher efficiency as well as better selectivity to Hg^{2+} than Ca^{2+} , Sr^{2+} , Mn^{2+} , Cr^{3+} , and especially Pb^{2+} and Cd^{2+} . Moreover, in the presence of PDCA, the LOD was further improved down to 100 nM, meaning that a short chain of mercapto aliphatic acid performed better in Hg^{2+} sensing. Functional molecule-AuNP systems circumvent complicated syntheses in producing oligonucleotides or oligopeptides.

Taking advantage of the greater thiophilic tendency of Hg^{2+} compared to other metal ions such as Pb^{2+} , Cd^{2+} , and Cu^{2+} , Kim et al. reported an attractive colorimetric sensor for Hg^{2+} detection through an S- Hg^{2+} -S interaction in a dithioerythritol (DTET)-modified AuNP system.^[60] In phosphate buffer (10 mM, pH 6.6), the DTET-AuNPs exhibited an obvious colorimetric response from red (525 nm) to blue (670 nm) upon addition of Hg^{2+} . Only two interfering ions were found: Cu^{2+} and Ba^{2+} led to a slow precipitation of AuNPs (over several hours), which could be masked by the addition of ethylene diamine tetraacetic acid (EDTA). The system showed a linear correlation between $E_{x_{670\text{ nm}/525\text{ nm}}}$ (the ratio of absorption coefficients at 670 nm and 525 nm) and Hg^{2+} concentration from the LOD of 100 nM to 600 nM ($R^2 = 0.9975$).

Furthermore, it was found that the combination of ligands supplied better performance toward specific metal ion detection. For instance, in an adenosine monophosphate (AMP)/MPA-AuNP system, AMP helped AuNPs disperse well in a highly saline solution due to electrostatic repulsion, while MPA was good at Hg^{2+} binding.^[61] Masking agents like PDCA are usually used to increase the selectivity in some assays, however, inspired by a good selectivity of thymine toward Hg^{2+} , a single thymine-involved derivative combined with a mercapto group was developed and functionalized on AuNPs for targeting Hg^{2+} (Figure 7).^[62] This probe showed excellent selectivity to Hg^{2+} due to the advantage of T- Hg^{2+} -T coordination chemistry, as well as a nanomolar level of LOD in tapwater samples without any masking agent.

Functional molecules can either stabilize the dispersion of nanoparticles for a red-to-blue sensing mode or, conversely, induce the aggregation of nanoparticles, which could be prevented by targets for a blue-to-red sensing mode. Indeed, Chen and Gao et al. found that 3-nitro-1*H*-1, 2, 4-triazole (NTA) could stabilize AuNPs against the aggregation induced by 2-amino-2-hydroxymethyl-propane-1,3-diol (Tris) (Figure 8).^[63] In the presence of Hg^{2+} , the NTA selectively bound Hg^{2+} , subsequently detached NTA from the surface of AuNPs, leading to Tris-induced aggregation of AuNPs. No noticeable color changes were observed in the presence of other metal ions at concentrations up to 100 mM in the absence of masking agents.

In the optimized conditions, the LODs of 7 nM and 50 nM were achieved by spectrophotometer and direct visualization, respectively. On the contrary, pyridine, 4,4-dipyridyl (DPY) and thymine were all good inducers of AuNP aggregation.^[64] Among the more common metal ions of Ca^{2+} , Cd^{2+} , Cr^{3+} , Co^{2+} , Cu^{2+} , Fe^{3+} , Hg^{2+} , Mg^{2+} , Mn^{2+} , Ni^{2+} , Pb^{2+} , Zn^{2+} and so on, only Hg^{2+} completely inhibited pyridine/DPY/thymine-induced nanoparticle aggregation via formation of pyridine/DPY/thymine- Hg^{2+} complexes. The LOD of DPY reached as low as 3.0 ppb because of its high affinity to Hg^{2+} , and 40 nM was the minimum level detected in tap-water and spring water samples.^[64a] Thymine did even better, for which an LOD of 0.4 ppb was obtained and recoveries of 88.0-112.5% were achieved in the application of Hg^{2+} assays in real water samples.^[64c]

5.2. Functional Chemodosimeter-AuNP Probes

In addition to the coordination interaction based strategies, the concepts and methodology of chemodosimeters^[65] can also be applied to AuNP-based colorimetric systems. For instance, thiourea derivatives have been developed as optical chemodosimeters for Hg^{2+} based on the Hg^{2+} induced desulfurization reaction with urea derivatives as products.^[66] Considering different behaviours of urea and thiourea toward AuNPs, Han et al. demonstrated a new type of unmodified AuNP system for Hg^{2+} detection with the assistance of a thiourea chemodosimeter.^[67] Thiourea derivatives could strongly adsorb on the surface of AuNPs (The $\log K_f$ of $\text{Au}(\text{SCN})_n$ is ca. 16.98,^[68]), which transformed nanoparticles from hydrophilic to hydrophobic and then induced their aggregation. After desulfurization, the product of urea loses this capability, so that the AuNP solution remained stable and red (Figure 9a).

The thiol group ($-\text{SH}$) is similar to the SCN group in that it can also bind AuNPs strongly. The $\log K_f$ of $\text{Hg}(\text{SCN})_n$ (ca. 21.8),^[68] however, exceeds that of $\text{Au}(\text{SCN})_n$, therefore, it is expected that only Hg^{2+} among metal ions has the ability to remove thiolates chemisorbed onto the surface of AuNPs (the $\log K_f$ values for Co^{2+} , Zn^{2+} , Cd^{2+} , Ni^{2+} , Pb^{2+} ,

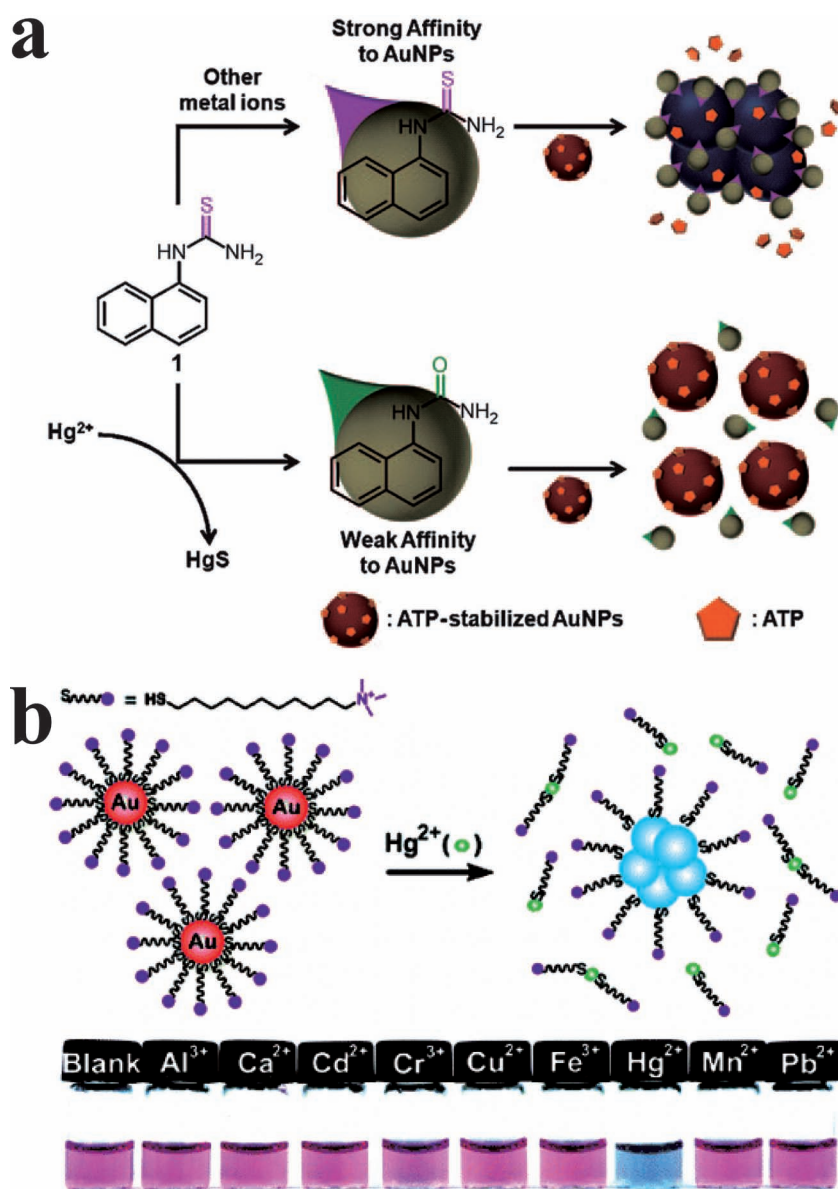


Figure 9. (a) Schematic representation of Hg^{2+} detection based on chemodosimeter-AuNPs system. Reproduced with permission.^[67]; and (b) schematic representation of proposed mechanism for the Hg^{2+} induced colorimetric response of QA-AuNP. Reproduced with permission.^[71] Copyright 2010, The American Chemical Society.

Mn^{2+} , Fe^{2+} , Fe^{3+} , Cr^{3+} , and Cu^{2+} are 1.72, 2.0, 2.8, 1.76, 1.48, 1.23, 1.31, 4.64, 3.08, and 10.4, respectively^[68]). To prove this strategy, Taki et al. modified AuNPs with HS-EG₃, in which a red color with an absorption peak at 520 nm was observed.^[69] Added Hg^{2+} broke the Au-S bonds prior to the aggregation process of AuNPs and this drastic red-to-blue color change only occurred with Hg^{2+} , but not Cu^{2+} , Co^{2+} , Mn^{2+} , Fe^{3+} , Ni^{2+} , Hg^{2+} , Pb^{2+} , Zn^{2+} , or Cd^{2+} . The extremely high affinity of the thiol group for Hg^{2+} once again explains this selective response. Later, Huang et al. studied AuNPs modified by alkanethiols with different chain lengths (2-mercaptoethanol, 4-mercaptobutanol, 6-mercaptohexanol, and 11-mercaptoundecanol), and they found that

the system of 4-mercaptobutanol-functionalized AuNPs showed best selectivity and sensitivity toward Hg^{2+} after a systematic comparison.^[70] Moreover, the introduction of quaternary ammonium ((11-mercapto-undecyl)-trimethylammonium) as a functionalizing agent could increase water solubility of the system to further bring better sensitivity (Figure 9b).^[71] Natural molecules with thiol groups, furthermore, are also applied in the examples of Hg^{2+} detection, which avoid complicated synthesis. For instance, the introduction of cysteine into a poly(diallyldimethylammonium) chloride-reduced AuNP solution aggregated the AuNPs and turned the solution color to purple, however, only Hg^{2+} can prevent this behavior due to the consumption of cysteine in the form of Hg^{2+} -cysteine complexes, in which the LOD achieved 25 nM.^[72]

An additional phenomenon could be used whereby surface-deposited Hg^{2+} on AuNPs could be reduced by a reducing agent, with mercury forming a solid amalgam-like structure on the surface of the AuNPs, leading to a decrease in SPR band intensity. As an illustrative example, Tseng et al. used Tween 20-capped AuNPs for the rapid and homogeneous detection of Hg^{2+}/Ag^+ .^[73] In this system, Tween 20 stabilized the particles against the high ionic strength, and the citrate reduced the Hg^{2+}/Ag^+ to form Hg/Ag -Au alloys which dislodged Tween 20 from the surface of AuNPs and then induced the aggregation of nanoparticles in highly ionic media (Figure 10a). With respect to Hg^{2+} detection, a masking agent such as NaCl (0.1 M) was introduced into the system to mask the effect from Ag^+ , leading to the precipitation of Ag^+ in the form of $AgCl$ (the solubility is 1.8×10^{-10}). Under optimum conditions (for Hg^{2+} : 0.24 nM Tween 20-AuNPs, 80 mM Na_3PO_4 , and 0.1 M NaCl), when the concentration of Hg^{2+} increased gradually from 0 to 1000 nM, an obvious colorimetric change occurred, from red to purple. There were good linear correlations between $Ex_{650\text{ nm}/520\text{ nm}}$ and Hg^{2+} concentration over 200–600 nM ($R^2 = 0.9944$) in drinking water and 300–1000 nM ($R^2 = 0.9977$) in sea water with LODs of 100 nM and 200 nM, respectively. Inspired by a similar strategy, Chen et al. presented a colorimetric method with a blue-to-red color change in the determination of Hg^{2+} and Ag^+ and a mechanism of stabilizing the AuNPs through a redox-formed metal coating with the help of ascorbic acid (AA). In the presence of Hg^{2+} or Ag^+ , the metal ions could be reduced by AA to form an Hg/Ag -Au

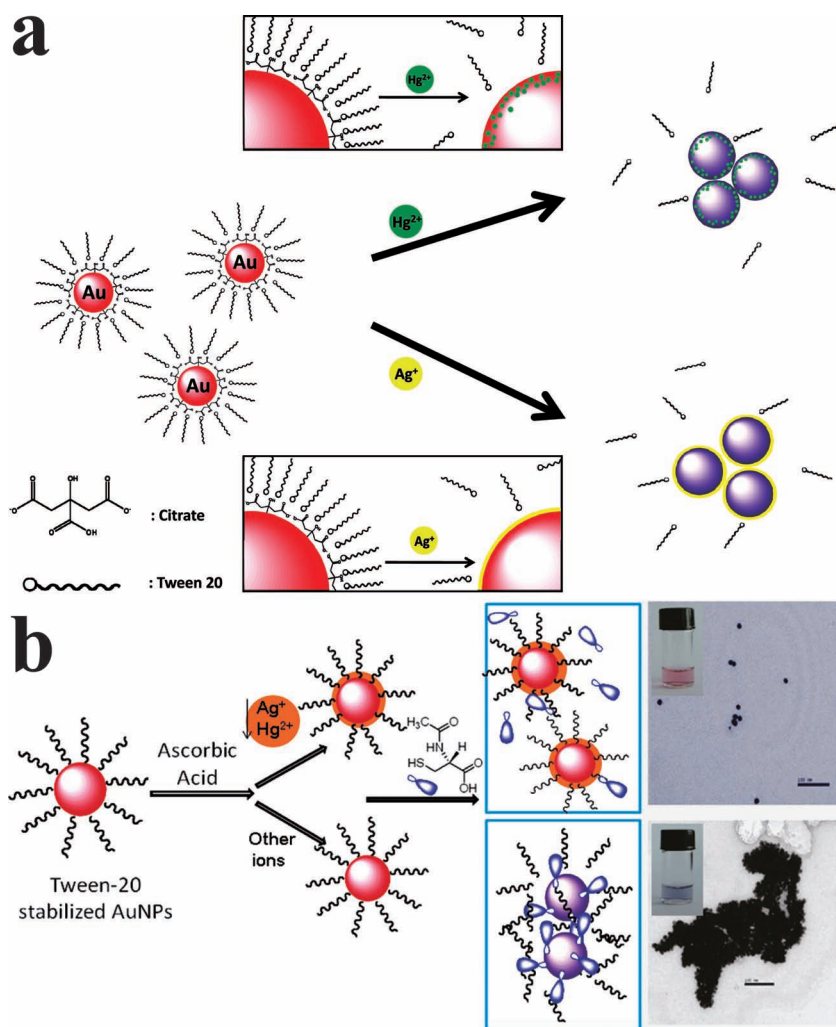


Figure 10. Illustration of the mechanism of (a) Tween 20- and (b) ascorbic acid-AuNP system for Hg^{2+} detection. Reproduced with permission.^[73,74] Copyright 2010 and 2011, The American Chemical Society.

alloy coating on the surface of AuNPs, which prevented the aggregation induced by self-assembling ligand *N*-acetyl-L-cysteine (Figure 10b).^[74] The examples above are based on the stronger oxidative ability of Hg^{2+} and Ag^+ compared to other metal ions.

6. Multiple Signal Amplification

AuNP-based colorimetric systems with high sensitivity need to be further explored to satisfy WHO standards. Therefore, methods where dual or even multiple signals are generated by coupling AuNPs with more sensitive signals as well as special structures or techniques, such as fluorescence,^[48] silver spot-based scattered light,^[75] hyper-Rayleigh scattering (HRS),^[76] unique core-shell nanostructures (Au@HgS),^[77] as well as immunoreaction-based lateral flow strip biocomponent (LFSB) technique^[78] and cloud point

extraction (CPE) technique,^[79] for augmenting signal sensitivity.

The sensitivity of AuNP-based colorimetric assays for Hg^{2+} detection using selective binding complexes of T- Hg^{2+} -T usually could not satisfy the aforementioned requirements. Therefore, utilizing a secondary amplification based on catalytic properties induced by nanoparticles, such as with the subsequent reduction of Ag^+ in the presence of hydroquinone provided a significantly increased sensitivity.^[75] Scattered light from silver spots was quickly measured with a Verigene Reader, in which the LOD reached 2 ppb (Figure 11a). In addition, the measurement of scattered light was more convenient. Ray et al. demonstrated a rapid, easy, and reliable method for Hg^{2+} detection based on the nonlinear optical (NLO) properties of MPA/HCys/PDCA-functionalized AuNPs.^[76] Hyper-Rayleigh scattering (HRS) technique can be used for monitoring NLO properties on the basis of light scattering. The HRS intensity of functionalized AuNPs varied with the addition of different amounts of Hg^{2+} , and the LOD could reach 5 ppb and 10 ppm by monitoring HRS and color change, respectively. Furthermore, the unique core-shell nanostructure (Au@HgS) was formed by the addition of Hg^{2+} into a AuNP-SH₂ complex solution, in which Hg^{2+} selectively reacted with H₂S on the surface of the AuNPs to form HgS quantum dots on the surface of the AuNPs. It was proved that this nanostructure could increase the SPR absorption due to the interaction of neighboring AuNPs and synergistic effects of the AuNPs with HgS, which supported this system's good LODs of 5 μM and 0.486 nM by the naked eye and UV-vis spectra, respectively.^[77] Besides the duplicate signal-amplifying methods, some other amplification techniques could be useful, such as immunoreaction-based LFSB technique and cloud point extraction of small-sized AuNPs. Based on the thymine-rich hairpin DNA-modified AuNP system and immunoreaction technique between digoxin and anti-digoxin antibodies on the LFSB, only the addition of Hg^{2+} can form duplex structures between hairpin DNA and digoxin-labeled DNA on the LFSB and produce a characteristic red band on the test zone for visual detection of Hg^{2+} .^[78] The sensitivity of this system can reach 0.1 nM, without instruments, with good selectivity. Another example of AuNP-based Hg^{2+} detection is developed on the basis of CPE,^[79] in which the extraction of PDCA-capped AuNPs (4 nm) into the Triton X-114 rich phase was so hard in the

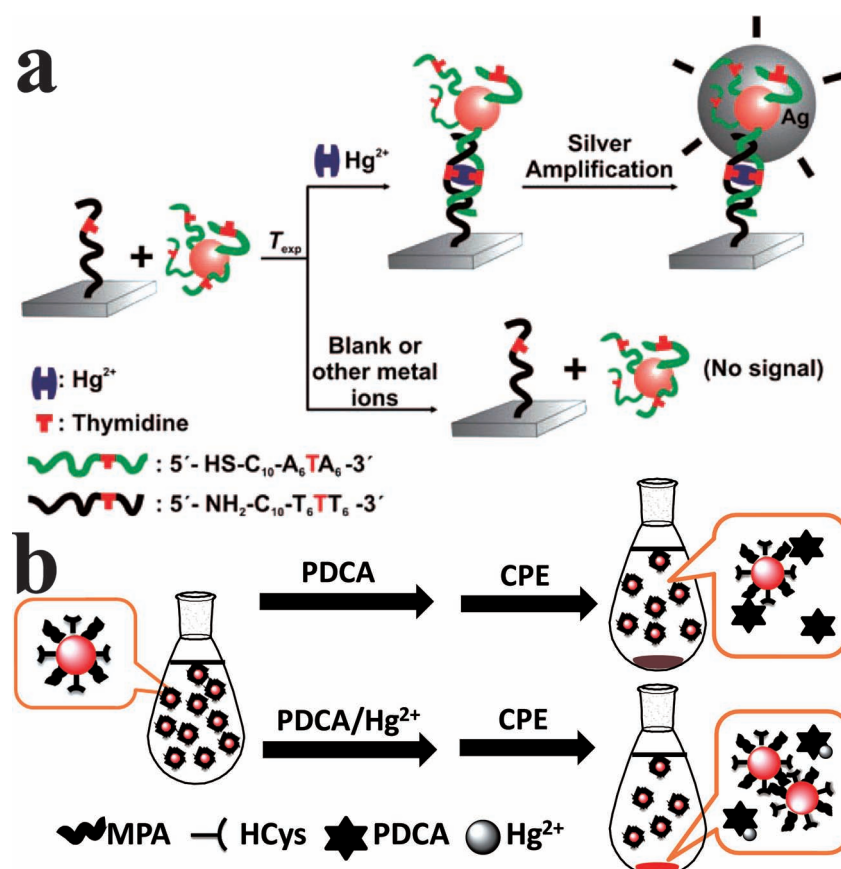


Figure 11. (a) Depiction of the chip-based scanometric detection of Hg²⁺ using DNA-AuNPs. Reproduced with permission.^[75] Copyright 2008, The American Chemical Society; and (b) schematic representation of Hg²⁺-triggered cloud point extraction of MPA/HCys-AuNPs for Hg²⁺ detection.

absence of Hg²⁺ that it was still colorless after the extraction (Figure 11b). In the presence of Hg²⁺, it was easy to get red Triton X-114 with rich AuNPs. Therefore, the visual and colorimetric detection of Hg²⁺ in the Triton X-114-rich phase was possible by the naked eye and UV-vis spectrophotometer, respectively. The introduction of MPA and HCys on the PDCA-capped AuNPs could further improve LODs to 5 ppb by the naked eye and 2 ppb by spectrophotometer, respectively, in optimum conditions (60 °C, 30 min). A linear range of 2-100 ppb (R² = 0.9975) was obtained by measuring the absorption at 520 nm in Triton X-114 phase.

7. Conclusion and Outlook

The application of AuNPs for colorimetric assays typically relies on strong coupling between the target analyte and nanoparticle, causing aggregation which, in turn, leads to a dramatic color change in the solution. This colorimetric “readout” circumvents the relative complexity inherent

in conventional optical imaging/detection methodologies and thus may prove to be suitable for low-cost point-of-care diagnostics. This review has presented various AuNP probes for the colorimetric detection of Hg²⁺ based on oligonucleotides, oligopeptides, and functional molecules in aqueous media. The key characteristics of each example, like selectivity, LOD, response time, and their applications in real samples are summarized in Table 1, which show competitive potential of AuNP-based assays. Colorimetric detection techniques are already commonly used for qualitative and even semi-quantitative analysis in labs (like pH test papers and temperature test papers) and even daily life (like urine test papers and pregnancy test strips). Though AuNPs are stable, biocompatible, and easy to prepare, store, functionalize in water, and test in in-the-field detecting applications, there still remain challenges to their application for the quantitative detection of environmental samples at the required LOD. Recent advances in smart-phone applications such as barcode recognition using cameras, sparked interesting ideas of using such devices as in-field detectors for instant diagnosis of blood or saliva, wherein merely a droplet is required on the phone's touch screen. Inspired by this concept, it is envisioned that a smart phone with software designed for colorimetric analysis could supply much more accurate and quantitative information supporting the qualitative judgement by the naked eye. Another example is the colorimetric analysis of our exhaled breath through an array of crossreactive plasmonic nanoparticles. It could be a fast, reliable, and portable diagnosis for lung cancer that could potentially provide early warnings to mitigate serious damage. It is exciting to imagine the frontiers of such paradigm-shifting applications, and we believe that plasmonic nanoparticle-based field assays and diagnoses could bring us a much more “colorful” and bright future.

Acknowledgements

We thank the financial support from SERC-TSRP (1021520015) and the National Research Foundation of Singapore (CREATE Programme of Nanomaterials for Energy and Water Management and NRF-RF2009-04).

Table 1. Key characteristics of AuNP-based probes for colorimetric detection of Hg²⁺.

Probe	LOD [nM]	Selectivity	Temperature/time	Real Sample	Reference
Oligonucleotide-AuNP Probes:					
DNA-AuNPs by Mirkin et al.	100	Hg ²⁺	47 °C	-	[41]
DNA-AuNPs by Liu et al.	1000	Hg ²⁺	RT (21.3 °C)	-	[44]
DNA-AuNPs by Takarada et al.	500	Hg ²⁺	RT and < 1 min	-	[46]
DNA attached AuPs by Yang et al.	-	Hg ^{2+a)}	RT and 30 min	Tap/lake water	[48]
T-rich DNA AuNPs by Willner et al.	10	Hg ^{2+a)}	RT and 20 min	-	[49]
T-rich DNA AuNPs by Yang et al.	200	Hg ^{2+a)}	RT and 30 min	Lake water	[50]
T ₃₃ DNA- AuNPs by Chang et al.	250	Hg ²⁺	RT and 10 min	-	[51]
T ₁₀ DNA-AuNPs by Li et al.	0.6	Hg ²⁺	RT and 10 min	Tap/lake water	[52]
T-rich DNA AuNPs by Li et al.	780	Hg ²⁺ and Pb ²⁺	RT and 30 min	-	[53]
T ₃₃ DNA-AuNPs by Tseng et al.	10	Hg ^{2+a)}	RT and 5 min	Pond water	[54]
Oligopeptide-AuNP Probes:					
Oligopeptide-AuNPs by Mandal et al.	2 × 10 ⁴	Hg ²⁺	RT and 10 min	-	[56]
Oligopeptide-AuNPs by Naik et al.	26	Hg ²⁺ , Co ²⁺ , Pd ²⁺ , Pd ⁴⁺ , Pt ²⁺	RT and <1 min	-	[57]
Oligopeptide-AuNPs by Chen et al.	10	Hg ²⁺	RT	-	[32]
Functional Molecule-AuNP Probes:					
11-mercaptoundecanoic AuNPs by Tupp et al.	-	Pb ²⁺ , Cd ²⁺ , Hg ²⁺	RT	-	[58]
MPA-AuNPs by Chang et al.	100	Hg ^{2+a)}	RT and <60 min	-	[59]
DTET-AuNPs by Kim et al.	100	Hg ^{2+a)}	RT and <10 min	-	[60]
MPA/AMP-AuNPs by Yu and Tseng et al.	500	Hg ²⁺	RT and 30 min	-	[61]
Thymine-SH AuNPs by Chen et al.	2.8	Hg ²⁺	RT and 5 min	Tap water	[62]
Tris/NTA-AuNPs by Chen and Gao et al.	7	Hg ²⁺	RT and 1 h	Lake water	[63]
DPY-AuNPs by Zhong et al.	15	Hg ²⁺	RT and 30 min	Tap/Spring water	[64a]
Pyridine-AuNPs by Tian et al.	55	Hg ²⁺	RT and <10 min	Tap water	[64b]
Thymine-AuNPs by Chen et al.	2	Hg ²⁺	RT and 30 min	Tap water	[64c]
Thiourea-AuNPs by Han et al.	193	Hg ²⁺ and Ag ⁺	RT and 3 min	-	[67]
HS-EG ₃ -AuNPs by Taki et al.	-	Hg ²⁺	RT and <30 min	-	[69]
4-Mercaptobutanol AuNPs by Huang et al.	500	Hg ²⁺	RT and 30 min	River water	[70]
MTA-AuNPs by Wang and Jiang et al.	30	Hg ²⁺	RT	-	[71]
Cysteine-AuNPs by Zhao, He, Zhang et al.	25	Hg ²⁺	RT	Drinking water	[72]
Tween 20-AuNPs by Tseng et al.	100	Hg ²⁺ and Ag ⁺	RT and 5 min	Drinking/sea water	[73]
AA-AuNPs by Chen et al.	5	Hg ²⁺ and Ag ⁺	RT and 3 min	Drinking/tap water	[74]
Multiple Signal Amplification Probes:					
Silver spot based scattered light-AuNPs by Mirkin et al.	10	Hg ²⁺	34 °C and 2 h	Lake water	[75]
HRS-AuNPs by Ray et al.	25	Hg ^{2+a)}	RT and 6-7 min	-	[76]
Au@HgS nanostructure by Wang, Wu et al.	0.486	Hg ²⁺	RT and 1.5 h	Pond water	[77]
Immunoreaction-AuNPs by He, Liu et al.	0.1	Hg ²⁺	RT and 20 min	Tap and River water	[78]
Cloud point extraction-AuNPs by Liu et al.	10	Hg ^{2+a)}	60 °C and 30 min	-	[79]

^{a)}Using PDCA as masking agent.

- [1] J. R. Miller, J. Rowland, P. J. Lechler, M. Desilets, L. C. Hsu, *Water Air Soil Poll.* **1996**, *86*, 373.
- [2] a) A. Renzoni, F. Zino, E. Franchi, *Environ. Res.* **1998**, *77*, 68; b) M. F. Wolfe, S. Schwarzbach, R. A. Sulaiman, *Environ. Toxicol. Chem.* **1998**, *17*, 146.
- [3] G. J. Burin, G. C. Becking, *Tr. Sub. Env.* **1991**, 207.
- [4] J. A. Moreton, H. T. Delves, *J. Anal. Atom. Spectrom.* **1998**, *13*, 659.
- [5] C. C. Wan, C. S. Chen, S. J. Jiang, *J. Anal. Atom. Spectrom.* **1997**, *12*, 683.
- [6] W. Geng, T. Nakajima, H. Takashi, A. Ohki, *J. Hazard. Mater.* **2008**, *154*, 325.
- [7] A. Ivask, T. Green, B. Polyak, A. Mor, A. Kahru, M. Virta, R. Marks, *Biosens. Bioelectron.* **2007**, *22*, 1396.
- [8] a) J. V. Ros-Lis, M. D. Marcos, R. Martinez-Manez, K. Rurack, J. Soto, *Angew. Chem. Int. Ed.* **2005**, *44*, 4405; b) Y. K. Yang, K. J. Yook, J. Tae, *J. Am. Chem. Soc.* **2005**, *127*, 16760; c) Z. Guo, W. H. Zhu, M. M. Zhu, X. M. Wu, H. Tian, *Chem. Eur. J.* **2010**, *16*, 14424; d) J. J. Du, J. L. Fan, X. J. Peng, P. P. Sun, J. Y. Wang, H. L. Li, S. G. Sun, *Org. Lett.* **2010**, *12*, 476.
- [9] a) I. B. Kim, U. H. F. Bunz, *J. Am. Chem. Soc.* **2006**, *128*, 2818; b) Y. L. Tang, F. He, M. H. Yu, F. D. Feng, L. L. An, H. Sun, S. Wang, Y. L. Li, D. B. Zhu, *Macromol. Rapid Commun.* **2006**, *27*, 389; c) J. Lee, H. Jun, J. Kim, *Adv. Mater.* **2009**, *21*, 3674.
- [10] a) P. Chen, C. A. He, *J. Am. Chem. Soc.* **2004**, *126*, 728; b) K. Hakila, T. Green, P. Leskinen, A. Ivask, R. Marks, M. Virta, *J. Appl. Toxicol.* **2004**, *24*, 333.
- [11] a) B. Chen, Y. Ying, Z. T. Zhou, P. Zhong, *Chem. Lett.* **2004**, *33*, 1608; b) C. Q. Zhu, L. Li, F. Fang, J. L. Chen, Y. Q. Wu, *Chem. Lett.* **2005**, *34*, 898.
- [12] P. Goldberg-Oppenheimer, S. Cosnier, R. S. Marks, O. Regev, *Talanta* **2008**, *75*, 1324.
- [13] a) H. J. Kim, D. S. Park, M. H. Hyun, Y. B. Shim, *Electroanal.* **1998**, *10*, 303; b) M. A. Nolan, S. P. Kounaves, *Anal. Chem.* **1999**, *71*, 3567.
- [14] a) J. F. Zhang, Y. Zhou, J. Yoon, J. S. Kim, *Chem. Soc. Rev.* **2011**, *40*, 3416; b) T. Q. Duong, J. S. Kim, *Chem. Rev.* **2010**, *110*, 6280.
- [15] a) R. M. Duke, E. B. Veale, F. M. Pfeffer, P. E. Kruger, T. Gunnlaugsson, *Chem. Soc. Rev.* **2010**, *39*, 3936; b) M. E. Moragues, R. Martinez-Manez, F. Sancenon, *Chem. Soc. Rev.* **2011**, *40*, 2593; c) R. Martinez-Manez, F. Sancenon, *Chem. Rev.* **2003**, *103*, 4419.
- [16] X. Chen, Y. Zhou, X. J. Peng, J. Yoon, *Chem. Soc. Rev.* **2010**, *39*, 2120.
- [17] Y. Zhou, J. Yoon, *Chem. Soc. Rev.* **2012**, *41*, 52.
- [18] Y. Zhou, Z. Xu, J. Yoon, *Chem. Soc. Rev.* **2011**, *40*, 2222.
- [19] Y. Salinas, R. Martinez-Manez, M. D. Marcos, F. Sancenon, A. M. Costero, M. Parra, S. Gil, *Chem. Soc. Rev.* **2012**, *41*, 1261.
- [20] a) C. Suksai, T. Tuntulani, *Chem. Soc. Rev.* **2003**, *32*, 192; b) W. S. Han, H. Y. Lee, S. H. Jung, S. J. Lee, J. H. Jung, *Chem. Soc. Rev.* **2009**, *38*, 1904.
- [21] a) K. L. Kelly, E. Coronado, L. L. Zhao, G. C. Schatz, *J. Phys. Chem. B* **2003**, *107*, 668; b) A. J. Haes, C. L. Haynes, A. D. McFarland, G. C. Schatz, R. R. Van Duyne, S. L. Zou, *MRS Bull.* **2005**, *30*, 368; c) K. A. Willets, R. P. Van Duyne, *Annu. Rev. Phys. Chem.* **2007**, *58*, 267.
- [22] a) Y. N. Xia, N. J. Halas, *MRS Bull.* **2005**, *30*, 338; b) C. Noguez, *J. Phys. Chem. C* **2007**, *111*, 3806.
- [23] a) N. L. Rosi, C. A. Mirkin, *Chem. Rev.* **2005**, *105*, 1547; b) L. X. Qin, Y. Li, D. W. Li, C. Jing, B. Q. Chen, W. Ma, A. Heyman, O. Shoseyov, I. Willner, H. Tian, Y. T. Long, *Angew. Chem. Int. Ed.* **2012**, *51*, 140; c) J. J. Zhang, M. Riskin, R. Freeman, R. Tel-Vered, D. Balogh, H. Tian, I. Willner, *ACS Nano* **2011**, *5*, 5936; d) B. Leng, L. Zou, J. B. Jiang, H. Tian, *Sensor Actuat B-Chem.* **2009**, *140*, 162; e) Z. Krpetic, P. Nativo, I. A. Prior, M. Brust, *Small* **2011**, *7*, 1982.
- [24] a) R. Elghanian, J. J. Storhoff, R. C. Mucic, R. L. Letsinger, C. A. Mirkin, *Science* **1997**, *277*, 1078; b) T. A. Taton, C. A. Mirkin, R. L. Letsinger, *Science* **2000**, *289*, 1757; c) W. Xu, X. J. Xue, T. H. Li, H. Q. Zeng, X. G. Liu, *Angew. Chem. Int. Ed.* **2009**, *48*, 6849; d) W. Xu, X. J. Xie, D. W. Li, Z. Q. Yang, T. H. Li, X. G. Liu, *Small* **2012**, *8*, 1846; e) X. J. Xue, W. Xu, F. Wang, X. G. Liu, *J. Am. Chem. Soc.* **2009**, *131*, 11668.
- [25] a) Y. Choi, N. H. Ho, C. H. Tung, *Angew. Chem. Int. Ed.* **2007**, *46*, 707; b) W. A. Zhao, W. Chiuman, J. C. F. Lam, M. A. Brook, Y. F. Li, *Chem. Commun.* **2007**, 3729; c) X. J. Xie, W. Xu, T. H. Li, X. G. Liu, *Small* **2011**, *7*, 1393.
- [26] S. Chah, M. R. Hammond, R. N. Zare, *Chem. Biol.* **2005**, *12*, 323.
- [27] a) M. S. Han, A. K. R. Lytton-Jean, C. A. Mirkin, *J. Am. Chem. Soc.* **2006**, *128*, 4954; b) X. Y. Xu, M. S. Han, C. A. Mirkin, *Angew. Chem. Int. Ed.* **2007**, *46*, 3468; c) J. Zhang, L. H. Wang, D. Pan, S. P. Song, F. Y. C. Boey, H. Zhang, C. H. Fan, *Small* **2008**, *4*, 1196; d) X. Xie, W. Xu, X. Liu, *Acc. Chem. Res.* **2012**, DOI: 10.1021/ar300044j.
- [28] a) A. J. Reynolds, A. H. Haines, D. A. Russell, *Langmuir* **2006**, *22*, 1156; b) W. R. Yang, J. J. Gooding, Z. C. He, Q. Li, G. N. Chen, *J. Nanosci. Nanotechnol.* **2007**, *7*, 712; c) H. B. Wang, W. Xu, H. Zhang, D. W. Li, Z. Q. Yang, X. J. Xie, T. H. Li, X. G. Liu, *Small* **2011**, *7*, 1987; d) J. J. Du, Q. Shao, S. Y. Yin, L. Jiang, J. Ma, X. D. Chen, *Small* **2012**, DOI: 10.1002/smll.201201650.
- [29] a) L. Jiang, Y. H. Sun, F. W. Huo, H. Zhang, L. D. Qin, S. Z. Li, X. D. Chen, *Nanoscale* **2012**, *4*, 66; b) L. Jiang, Y. H. Sun, C. Nowak, A. Kibrom, C. J. Zou, J. Ma, H. Fuchs, S. Z. Li, L. F. Chi, X. D. Chen, *ACS Nano* **2011**, *5*, 8288; c) B. J. Yang, N. Lu, D. P. Qi, R. P. Ma, Q. Wu, J. Y. Hao, X. M. Liu, Y. Mu, V. Reboud, N. Kehagias, C. M. S. Torres, F. Y. C. Boey, X. D. Chen, L. F. Chi, *Small* **2010**, *6*, 1038; d) X. D. Chen, S. Z. Li, C. Xue, M. J. Banholzer, G. C. Schatz, C. A. Mirkin, *ACS Nano* **2009**, *3*, 87.
- [30] a) M. R. Jones, K. D. Osberg, R. J. Macfarlane, M. R. Langille, C. A. Mirkin, *Chem. Rev.* **2011**, *111*, 3736; b) K. Saha, S. S. Agasti, C. Kim, X. Li, V. M. Rotello, *Chem. Rev.* **2012**, *112*, 2739.
- [31] C. Xue, C. A. Mirkin, *Angew. Chem. Int. Ed.* **2007**, *46*, 2036.
- [32] J. J. Du, Y. H. Sun, L. Jiang, X. B. Cao, D. P. Qi, S. Y. Yin, J. Ma, F. Y. C. Boey, X. D. Chen, *Small* **2011**, *7*, 1407.
- [33] a) C. A. Mirkin, R. L. Letsinger, R. C. Mucic, J. J. Storhoff, *Nature* **1996**, *382*, 607; b) J. J. Storhoff, C. A. Mirkin, *Chem. Rev.* **1999**, *99*, 1849.
- [34] a) R. Wilson, *Chem. Soc. Rev.* **2008**, *37*, 2028; b) W. Zhao, M. A. Brook, Y. F. Li, *ChemBioChem* **2008**, *9*, 2363; c) S. P. Song, Y. Qin, Y. He, Q. Huang, C. H. Fan, H. Y. Chen, *Chem. Soc. Rev.* **2010**, *39*, 4234; d) D. B. Liu, Z. Wang, X. Y. Jiang, *Nanoscale* **2011**, *3*, 1421.
- [35] a) C. M. Niemeyer, *Angew. Chem. Int. Ed.* **2001**, *40*, 4128; b) J. M. Nam, C. S. Thaxton, C. A. Mirkin, *Science* **2003**, *301*, 1884; c) V. Pavlov, Y. Xiao, B. Shlyahovsky, I. Willner, *J. Am. Chem. Soc.* **2004**, *126*, 11768; d) S. I. Stoeva, J. S. Lee, J. E. Smith, S. T. Rosen, C. A. Mirkin, *J. Am. Chem. Soc.* **2006**, *128*, 8378.
- [36] J. J. Storhoff, R. Elghanian, R. C. Mucic, C. A. Mirkin, R. L. Letsinger, *J. Am. Chem. Soc.* **1998**, *120*, 1959.
- [37] S. Y. Lin, S. H. Wu, C. H. Chen, *Angew. Chem. Int. Ed.* **2006**, *45*, 4948.
- [38] a) M. S. Han, A. K. R. Lytton-Jean, B. K. Oh, J. Heo, C. A. Mirkin, *Angew. Chem. Int. Ed.* **2006**, *45*, 1807; b) J. W. Liu, Y. Lu, *Angew. Chem. Int. Ed.* **2006**, *45*, 90.
- [39] S. Y. Park, A. K. R. Lytton-Jean, B. Lee, S. Weigand, G. C. Schatz, C. A. Mirkin, *Nature* **2008**, *451*, 553.
- [40] a) H. D. Hill, S. J. Hurst, C. A. Mirkin, *Nano Lett.* **2009**, *9*, 317; b) D. Nykpanchuk, M. M. Maye, D. van der Lelie, O. Gang, *Nature* **2008**, *451*, 549; c) S. J. Hurst, H. D. Hill, C. A. Mirkin, *J. Am. Chem. Soc.* **2008**, *130*, 12192.
- [41] J. S. Lee, M. S. Han, C. A. Mirkin, *Angew. Chem. Int. Ed.* **2007**, *46*, 4093.
- [42] J. S. Lee, P. A. Ulmann, M. S. Han, C. A. Mirkin, *Nano Lett.* **2008**, *8*, 529.
- [43] a) S. Katz, *J. Am. Chem. Soc.* **1952**, *74*, 2238; b) Y. Tanaka, S. Oda, H. Yamaguchi, Y. Kondo, C. Kojima, A. Ono, *J. Am. Chem. Soc.* **2007**, *129*, 244.

- [44] X. J. Xue, F. Wang, X. G. Liu, *J. Am. Chem. Soc.* **2008**, *130*, 3244.
- [45] J. H. Oh, J. S. Lee, *Anal. Chem.* **2011**, *83*, 7364.
- [46] N. Kanayama, T. Takarada, M. Maeda, *Chem. Commun.* **2011**, *47*, 2077.
- [47] H. X. Li, L. Rothberg, *Proc. Natl. Acad. Sci. USA* **2004**, *101*, 14036.
- [48] H. Wang, Y. X. Wang, J. Y. Jin, R. H. Yang, *Anal. Chem.* **2008**, *80*, 9021.
- [49] D. Li, A. Wieckowska, I. Willner, *Angew. Chem. Int. Ed.* **2008**, *47*, 3927.
- [50] Y. Wang, F. Yang, X. R. Yang, *Biosens. Bioelectron.* **2010**, *25*, 1994.
- [51] C. W. Liu, Y. T. Hsieh, C. C. Huang, Z. H. Lin, H. T. Chang, *Chem. Commun.* **2008**, 2242.
- [52] L. Li, B. X. Li, Y. Y. Qi, Y. Jin, *Anal. Bioanal. Chem.* **2009**, *393*, 2051.
- [53] X. B. Zuo, H. A. Wu, J. Toh, S. F. Y. Li, *Talanta* **2010**, *82*, 1642.
- [54] C. J. Yu, T. L. Cheng, W. L. Tseng, *Biosens. Bioelectron.* **2009**, *25*, 204.
- [55] B. P. Joshi, J. Park, W. I. Lee, K. H. Lee, *Talanta* **2009**, *78*, 903.
- [56] S. Si, A. Kotal, T. K. Mandal, *J. Phys. Chem. C* **2007**, *111*, 1248.
- [57] J. M. Slocik, J. S. Zabinski, D. M. Phillips, R. R. Naik, *Small* **2008**, *4*, 548.
- [58] Y. J. Kim, R. C. Johnson, J. T. Hupp, *Nano Lett.* **2001**, *1*, 165.
- [59] C. C. Huang, H. T. Chang, *Chem. Commun.* **2007**, 1215.
- [60] Y. R. Kim, R. K. Mahajan, J. S. Kim, H. Kim, *ACS Appl. Mater. Inter.* **2010**, *2*, 292.
- [61] C. J. Yu, W. L. Tseng, *Langmuir* **2008**, *24*, 12717.
- [62] L. Chen, T. T. Lou, C. W. Yu, Q. Kang, L. X. Chen, *Analyst* **2011**, *136*, 4770.
- [63] X. J. Chen, Y. B. Zu, H. Xie, A. M. Kemas, Z. Q. Gao, *Analyst* **2011**, *136*, 1690.
- [64] a) Y. Li, P. Wu, H. Xu, Z. P. Zhang, X. H. Zhong, *Talanta* **2011**, *84*, 508; b) X. R. Yang, H. X. Liu, J. Xu, X. M. Tang, H. Huang, D. B. Tian, *Nanotechnology* **2011**, *22*, 275503; c) T. T. Lou, L. Chen, C. R. Zhang, Q. Kang, H. Y. You, D. Z. Shen, L. X. Chen, *Anal. Methods* **2012**, *4*, 488.
- [65] J. J. Du, M. M. Hu, J. L. Fan, X. J. Peng, *Chem. Soc. Rev.* **2012**, *41*, 4511.
- [66] a) M. Y. Chae, A. W. Czarnik, *J. Am. Chem. Soc.* **1992**, *114*, 9704; b) X. L. Zhang, Y. Xiao, X. H. Qian, *Angew. Chem. Int. Ed.* **2008**, *47*, 8025.
- [67] S. Kim, N. H. Lee, S. H. Seo, M. S. Eom, S. Ahn, M. S. Han, *Chem. Asian J.* **2010**, *5*, 2463.
- [68] R. M. Smith, A. E. Martell, *Sci. Total Environ.* **1987**, *64*, 125.
- [69] T. Hirayama, M. Taki, Y. Kashiwagi, M. Nakamoto, A. Kunishita, S. Itoh, Y. Yamamoto, *Dalton Trans.* **2008**, 4705.
- [70] Y. L. Hung, T. M. Hsiung, Y. Y. Chen, Y. F. Huang, C. C. Huang, *J. Phys. Chem. C* **2010**, *114*, 16329.
- [71] D. B. Liu, W. S. Qu, W. W. Chen, W. Zhang, Z. Wang, X. Y. Jiang, *Anal. Chem.* **2010**, *82*, 9606.
- [72] N. Ding, H. Zhao, W. B. Peng, Y. J. He, Y. Zhou, L. F. Yuan, Y. X. Zhang, *Colloid Surface A* **2012**, *395*, 161.
- [73] C. Y. Lin, C. J. Yu, Y. H. Lin, W. L. Tseng, *Anal. Chem.* **2010**, *82*, 6830.
- [74] T. T. Lou, Z. P. Chen, Y. Q. Wang, L. X. Chen, *ACS Appl. Mater. Inter.* **2011**, *3*, 1568.
- [75] J. S. Lee, C. A. Mirkin, *Anal. Chem.* **2008**, *80*, 6805.
- [76] G. K. Darbha, A. K. Singh, U. S. Rai, E. Yu, H. T. Yu, P. C. Ray, *J. Am. Chem. Soc.* **2008**, *130*, 8038.
- [77] F. Q. Zhang, L. Y. Zeng, C. Yang, J. W. Xin, H. Y. Wang, A. G. Wu, *Analyst* **2011**, *136*, 2825.
- [78] Y. Q. He, X. B. Zhang, K. Zeng, S. Q. Zhang, M. Baloda, A. S. Gurung, G. D. Liu, *Biosens. Bioelectron.* **2011**, *26*, 4464.
- [79] Z. Q. Tan, J. F. Liu, R. Liu, Y. G. Yin, G. B. Jiang, *Chem. Commun.* **2009**, 7030.

Received: April 16, 2012
Published online: September 7, 2012